Enterocyte loss of polarity and gut wound healing rely upon the F-actin–severing function of villin

Florent Ubelmann[a], Mathias Chamaillard[b], Fatima El-Marjou[a], Anthony Simon[a], Jeanne Netter[a], Danijela Vignjevic[a], Buford L. Nichols[c], Roberto Quezada-Calvillo[c], Teddy Grandjean[b], Daniel Louvard[a,1], Céline Revenu[a,1,2,3], and Sylvie Robine[a,1,3]

[a]Unité Mixte de Recherche 144, Centre National de la Recherche Scientifique, Institut Curie, 75248 Paris Cedex 05, France; [b]Center for Infection and Immunity of Lille, Institut National de la Santé et Recherche Médicale U1019/Centre National de la Recherche Scientifique Unité Mixte de Recherche 8204, Institut Pasteur Lille, 59019 Lille Cedex, France; [c]United States Department of Agriculture Agricultural Research Service Children's Nutrition Research Center, Department of Pediatrics, Baylor College of Medicine, Houston, TX 77030

Edited by Mina J. Bissell, E. O. Lawrence Berkeley National Laboratory, Berkeley, CA, and approved February 22, 2013 (received for review October 24, 2012)

Efficient wound healing is required to maintain the integrity of the intestinal epithelial barrier because of its constant exposure to a large variety of environmental stresses. This process implies a partial cell depolarization and the acquisition of a motile phenotype that involves rearrangements of the actin cytoskeleton. Here we address how polarized enterocytes harboring actin-rich apical microvilli undergo extensive cell remodeling to drive injury repair. Using live imaging technologies, we demonstrate that enterocytes in vitro and in vivo rapidly depolarize their microvilli at the wound edge. Through its F-actin–severing activity, the microvillar actin-binding protein villin drives both apical microvilli disassembly in vitro and in vivo and promotes lamellipodial extension. Photoactivation experiments indicate that microvillar actin is mobilized at the lamellipodium, allowing optimal migration. Finally, efficient repair of colonic mechanical injuries requires villin severing of F-actin, emphasizing the importance of villin function in intestinal homeostasis. Thus, villin severs F-actin to ensure microvillus depolarization and enterocyte remodeling upon injury. This work highlights the importance of specialized apical pole disassembly for the repolarization of epithelial cells initiating migration.

intestine | actin dynamics

Epithelia constitute the interface between an organ or organism and its environment. This interface ensures a selective barrier that allows the necessary exchanges with the external milieu while guaranteeing protection from external threats. This barrier is made possible by the apico-basal polarization of cells, which involves the tight sealing of neighboring cells via cell–cell junctions. The digestive epithelium consists of a monostratified layer of differentiated epithelial cells. The vast majority of differentiated intestinal cells are columnar enterocytes, which represent the archetype of cellular apico-basal polarity. The enterocyte apex is covered by numerous microvilli, which are microscopic membrane protrusions structured by a network of uniformly polarized actin filaments organized by actin-binding proteins. Their membrane, highly enriched in hydrolases, channels and peptide transporters, endows the cells with an immense digestive and absorptive capacity. Thus, the presence of microvilli morphologically and functionally defines the apical pole of intestinal epithelial cells.

The intestinal epithelium continuously faces assaults induced by dietary products, bile salts, xenobiotics, and pharmaceuticals, which can result in wounding of the epithelium. For efficient epithelial healing, the migration of cells adjacent to the wound allows the rapid reconstitution of epithelial integrity. The migration of the adjacent intact monolayer rapidly restores the barrier function of the epithelium in a process termed "restitution" (1–3), which involves the collective movement of cells that remain in contact with their neighbors during migration. During this process an important cellular reorganization occurs whereby cells acquire a front/rear polarity and actin-rich migratory structures while preserving cell–cell junctions and epithelial integrity (4–6). The actin cytoskeleton largely participates in cell architecture and is particularly involved in the junctional and apical organization of epithelial cells (7, 8) and in the establishment and dynamics of the locomotion machinery (9). Thus, the local architecture of the actin cytoskeleton and its remodeling constitute major parameters that require tight regulation to allow the cell morphological changes that enable the epithelial reorganization necessary for cell migration.

The external cues and signaling molecules that trigger the cell remodeling associated with restitution are relatively well known (e.g., Rho, Rac, and Trefoil factors); however, the molecular effectors require further characterization (10–15). Because of the highly characteristic apico-basal polarity of enterocytes and their highly differentiated state, the intestinal epithelium is particularly well suited to the study of epithelial remodeling and the underlying actin cytoskeletal reorganization required for wound repair. Among the molecular candidates, villin is an actin-binding protein that concentrates in microvilli and is expressed predominantly in the digestive tract. This protein bundles, caps, and severs actin filaments in vitro in a calcium-dependent manner (16–18). Its severing activity is favored in vitro by the phosphorylation of several tyrosine residues (19). Villin has a prominent function in colonic wound repair and mouse survival

Significance

Intestinal epithelium damage is common but becomes recurrent in chronic intestinal disorders. Healing implies cell migration, which necessitates extensive cellular reorganization. We demonstrate that intestinal epithelial cells completely disassemble their apical actin-based microvilli upon migration, and we identify the protein villin and its actin-severing function as responsible for this physiological process. We show that this apical pole effacement is required for the acquisition of a motile phenotype and efficient wound healing. These findings demonstrate how intestinal epithelial cells acquired a mechanism at the level of the actin cytoskeleton to convert efficiently from a highly differentiated to a motile polarity.

Author contributions: F.U., M.C., D.V., D.L., C.R., and S.R. designed research; F.U., M.C., A.S., J.N., T.G., and C.R. performed research; F.U., F.E.-M., D.V., B.L.N., and R.Q.-C. contributed new reagents/analytic tools; F.U., M.C., A.S., C.R., and S.R. analyzed data; and F.U., D.L., C.R., and S.R. wrote the paper.

The authors declare no conflict of interest.

This article is a PNAS Direct Submission.

[1]To whom correspondence may be addressed. E-mail: daniel.louvard@curie.fr, revenu@embl.de, or Sylvie.Robine@curie.fr.

[2]Present address: European Molecular Biology Laboratory, 69126 Heidelberg, Germany.

[3]C.R. and S.R. contributed equally to this paper.

This article contains supporting information online at www.pnas.org/lookup/suppl/doi:10.1073/pnas.1218446110/-/DCSupplemental.

in a model of experimentally induced colitis (20); however, the cellular mechanisms underlying villin function in these processes remain unclear and controversial. An antiapoptotic role ensuring epithelial protection against lesions has been proposed (21). Alternatively, villin may favor the actin and cell plasticity, which are required during mucosal healing (20). Indeed villin localizes at the lamellipodium of migrating cells and also enhances migration in numerous cell lines (22–25). Moreover, the actin severing mediated by villin has been shown to enhance the actin-based motility of beads in vitro and of bacteria in infected cells (26).

Villin is present exclusively in epithelial cells with extensively developed microvilli and is, therefore, likely to have a specific function associated with this specialized organelle. In this study, we investigated the changes in cell shape during intestinal epithelial restitution and directly tested the impact of villin's severing function in epithelial resealing in vivo. We take advantage of an extensively characterized villin mutant affected only in its severing property (26), together with live imaging of cells in culture and in vivo to investigate enterocyte remodeling during wound healing.

Results

Villin Accelerates Colonic Wound Healing Independently of Apoptosis and Proliferation. Villin has been proposed to be involved in cellular plasticity and survival after the induction of colonic lesions by dextran sulfate sodium salt (20, 21). However, the high level of apoptosis in this system hinders a precise analysis of epithelial restitution. To clarify unambiguously whether villin participates in gut wound healing independently of any antiapoptotic role, we mechanically injured mouse colonic mucosa to minimize potential biological side effects of more classical chemical injuries. We used size 3-French biopsy forceps to create a discrete, round injury in the distal mouse colon (27, 28) and used an endoscopic system dedicated to small animals to evaluate the mucosal repair process at days 3 and 7 postinjury with careful quantitative measurements of the injured area. WT mice consistently showed a substantial reduction in the ulcerated area at day 3 (Fig. 1*B*). By day 7, the colon surface appeared regular, and the original lesion was almost indistinguishable (Fig. 1*A*). In contrast, colonic repair in villin-null mice was slightly delayed at day 3 (Fig. 1*B*), and at day 7 the strikingly irregular and depressed appearance of the tissue indicated incomplete mucosal healing (Fig. 1*A*). Quantification confirmed slower healing in villin-null mice with a significantly slower reduction in the surface area of the injury than seen in WT animals (69 ± 7 vs. 54 ± 10 at day 3, and 56 ± 9 vs. 17 ± 3 at day 7; $P < 0.05$ at day 7; Wilcoxon rank sum test) (Fig. 1*B*). Thus, efficient colonic wound healing requires villin in vivo. Studies of the repair process were carried out on colonic paraffin sections corresponding to injuries previously identified by colonoscopy at day 4, when significant differences arise between WT and villin-null animals. To investigate the effects of villin on cell proliferation and apoptosis during mucosal healing, we evaluated these processes using immunohistochemistry (Fig. 1*C*). Costaining for E-cadherin and the ki-67 proliferation marker did not reveal any major difference in terms of cell proliferation. Furthermore, the number of cells colabeled with E-cadherin and cleaved caspase 3 was not greater in WT animals than in villin-null mice. Thus, villin's role in cell proliferation or apoptosis was not responsible for the delayed wound healing in villin-knockout mice.

Generation and Characterization of Monomeric Cherry-Villin Transgenic Mouse Models. To decipher the molecular mechanism by which villin fulfills its function, we decided to study the contribution of its F-actin–severing function during wound healing by expressing fluorescently tagged villin WT or mutated proteins in mouse enterocytes. Inducible transgenic targeting vectors containing floxed monomeric Cherry-villin WT (mCherry-villinWT) or a previously described mCherry-villin selectively mutated for its F-actin–severing property (mCherry-villinΔsev) (26) under a chicken β-actin hybrid (CAG) ubiquitous promoter were constructed (Fig. S1). Using Speedy Mouse technology, we generated mouse models carrying a single copy of the transgene inserted in the hypoxanthine-guanine phosphoribosyltransferase (*HPRT*) locus. By successive crosses with mice expressing a tamoxifen-inducible Cre recombinase expressed

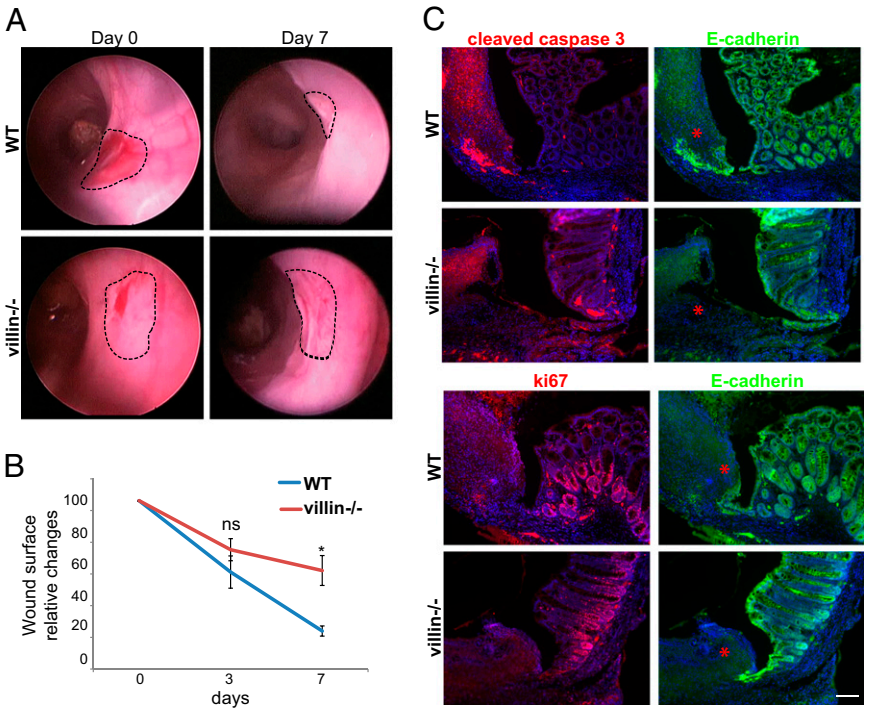

Fig. 1. Efficient colonic wound healing requires villin. (*A*) Serial endoscopic snapshots showing the site of biopsy-induced injury in mouse colon of the indicated genotypes at day 0 and 7 after wounding. Images are representative of at least four animals per genotype. Dashed lines delineate the wounded area. (*B*) Plot of the average changes in the wounded area over time for mice of the indicated genotype, normalized to the original lesion size at day 0. Values are for WT and villin$^{-/-}$ mice, respectively. Day 3: 54 ± 10 vs. 69 ± 7%; day 7: 17 ± 3 vs. 56 ± 9%. WT: $n = 6$; villin$^{-/-}$: $n = 4$. Wilcoxon; *$P < 0.05$, NS, nonsignificant ($P > 0.05$). (*C*) Histological sections from WT and villin$^{-/-}$ mice, at day 4 postinjury stained for cleaved caspase 3 (*Upper Left*, red) or ki67 (*Lower Left*, red) and E-cadherin (*Upper and Lower Right*, green). DAPI stains nuclei (blue). Red asterisks highlight the injured area. (Scale bar: 100 μm.)

under the control of the villin promoter (referred to as "villin: creERT2") (29) in a villin-null background (20), we generated villin-null mice carrying either mCherry-villinWT and villin: creERT2 transgenes (tgvillinWT) or mCherry-villinΔsev and villin:creERT2 transgenes (tgvillinΔsev) to study the function of villin and its severing mutant in the absence of endogenous villin. After tamoxifen induction, villin protein expression analyzed by Western blot on total cell extracts from jejunal and colonic tissues revealed a single band of ~120 kDa, with comparable levels found for both tgvillinWT and tgvillinΔsev mice (Fig. S2*A*). This molecular mass corresponds to villin (92.5 kDa) fused to the mCherry protein (~30 kDa). We noticed a slight decrease in transgenic villin levels compared with endogenous villin expression (Fig. S2*A*). To evaluate the cellular distribution of both transgenic proteins, we analyzed the mCherry fluorescence on frozen histological sections. We found a homogeneous signal along the villus axis in the small intestine and in the colonic epithelium (Fig. 2*A*). This distribution is similar to the distribution of endogenous villin (30). At higher magnification, we observed a strong apical concentration of the mCherry-fused proteins on the enterocytes colocalizing with the intense apical F-actin signal at the brush border, as expected for villin expression (Fig. S2 *B* and *C*, *Upper*). Thus, we conclude that the two mouse models recapitulate the expression and localization of the endogenous villin protein.

Efficient Wound Healing in the Mouse Colon Requires F-Actin Severing by Villin. To assess in vivo the functionality of the transgenic proteins, we performed basolateral infusion of carbachol on isolated intestinal segments. This procedure is known to increase intracellular calcium and to induce the loss of microvillus F-actin in a villin-dependent manner (20). After carbachol treatment, the remaining apical F-actin corresponds to the terminal web and junctional actin belt region of the enterocyte, which has lost its normal brush border. After the carbachol infusion procedure, we analyzed the F-actin distribution in enterocytes using phalloidin staining of histological sections. As previously described (20), the broad apical F-actin labeling typical of normal enterocytes was essentially lost on carbachol-treated WT animals, indicating disruption of the brush border (Fig. 2*B*). Quantification of the width of apical F-actin staining demonstrated strongly reduced staining in treated animals (2.28 ± 0.08 μm vs. 0.54 ± 0.07 μm, $P < 0.001$, *t* test) (Fig. 2*D*). In contrast, the broad apical F-actin labeling was preserved on treated villin-knockout animals (2.34 ± 0.07 μm vs. 2.20 ± 0.10 μm, $P > 0.5$, *t* test) (Fig. 2 *B* and *D*). Importantly, carbachol exposure of tgvillinWT intestinal segments led to a striking reduction in the width of apical F-actin staining (2.10 ± 0.09 μm vs. 0.68 ± 0.05 μm, $P < 0.001$, *t* test), restoring the WT behavior (Fig. 2 *C* and *D*). Thus, the mCherry-villinWT protein is functional in vivo and is able to rescue the loss of endogenous villin. Conversely, carbachol-treated tgvillinΔsev mice did not demonstrate any alteration in apical phalloidin staining of enterocytes (2.08 ± 0.08 μm vs. 1.92 ± 0.15 μm, $P > 0.5$, *t* test) (Fig. 2 *C* and *D*). These results validate the functionality of the transgenic proteins in the newly generated mouse models and demonstrate that villin mediates carbachol-induced microvillar F-actin disassembly through its severing property in vivo.

Having generated the proper tools to determine whether the actin-severing property of villin is important for colonic tissue healing, we then monitored in vivo the injury repair process in tgvillinΔsev and tgvillinWT mice. In tgvillinWT animals, most of the original wound was repaired by day 7 (Fig. 3*A*), mimicking the WT mouse phenotype. On the contrary, injuries induced on tgvillinΔsev mice failed to heal properly at days 3 (Fig. 3*B*) and 7 (Fig. 3*A*). We confirmed these observations by comparing the injured surface area over time in tgvillinΔsev and tgvillinWT mice (74 ± 8 vs. 57 ± 6% at day 3 and 62 ± 5 vs. 17 ± 7% at day 7, $P < 0.05$ for day 7, Wilcoxon rank sum test) (Fig. 3*B*). Together, these results demonstrate the critical role of villin-mediated F-actin severing during colonic injury repair independently of an antiapoptotic function in vivo. Given the known impact of villin on cell migration, we subsequently decided to analyze the migratory properties of epithelial cells in detail.

Villin's Severing Activity Is Required for Efficient Wound Healing of LLC-PK1 Cells. To analyze the dynamics of the healing process at the cellular level, we turned to wound-healing models in cell

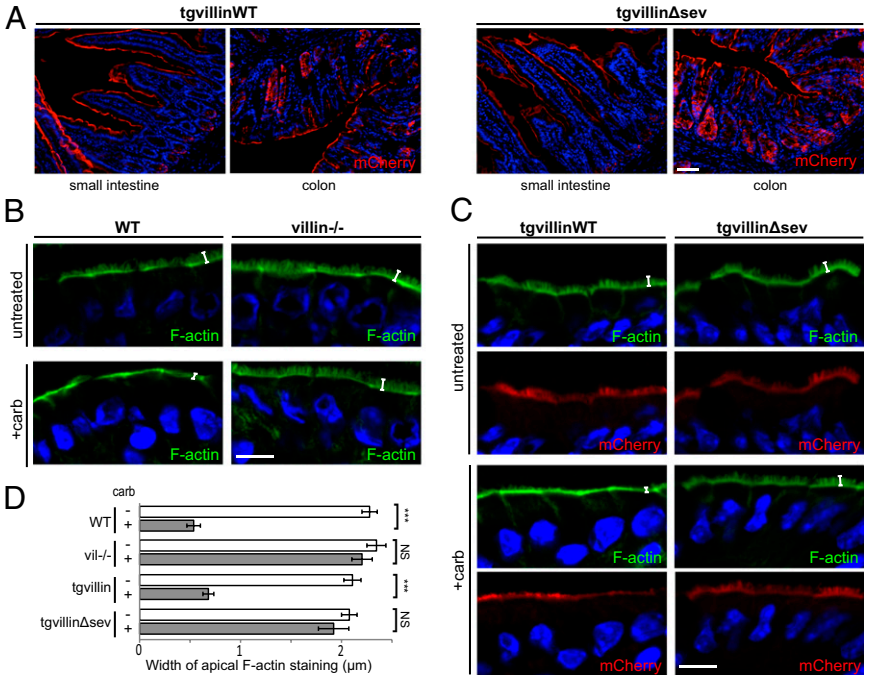

Fig. 2. Transgenic villin proteins are functional, and villin severing activity is required for brush border disassembly upon carbachol treatment in vivo. (*A*) Histological frozen sections from jejunum (*Left*) or colon (*Right*) of tgvillinWT or tgvillinΔsev mice showing villin-mCherry fluorescence (red). DAPI labels nuclei (blue). (Scale bar: 100 μm.) (*B* and *C*) Histological frozen sections from untreated or carbachol-treated (+carb) small intestines stained for F-actin by phalloidin (green). DAPI labels nuclei (blue). White brackets indicate the width of the F-actin concentration at the apex of the enterocytes. (*B*) Sections from WT or villin$^{-/-}$ mice. (*C*) Sections from tgvillinWT or tgvillinΔsev mice. mCherry-villin fluorescence is shown (red). (Scale bar: 10 μm.) (*D*) Histogram depicting the width of the apical F-actin concentration of WT, villin$^{-/-}$, tgvillinWT, or tgvillinΔsev mice untreated or treated with carbachol. Width values (in μm) are WT, 2.28 ± 0.08; WT+carb: 0.54 ± 0.07; villin$^{-/-}$, 2.35 ± 0.09; villin$^{-/-}$+carb, 2.20 ± 0.10; tgvillinWT, 2.10 ± 0.09; tgvillinWT+carb, 0.68 ± 0.05; tgvillinΔsev, 2.08 ± 0.08; tgvillinΔsev+carb, 1.92 ± 0.15. Numbers of measurements are WT: untreated; $n = 15$; WT+carb: $n = 15$; villin$^{-/-}$ untreated: $n = 8$; villin$^{-/-}$+carb: $n = 16$; tgvillinWT: $n = 11$; tgvillinWT+carb: $n = 44$; tgvillinΔsev, $n = 15$; tgvillinΔsev+carb: $n = 45$. ***$P < 0.001$; NS, nonsignificant ($P > 0.05$ *t* test).

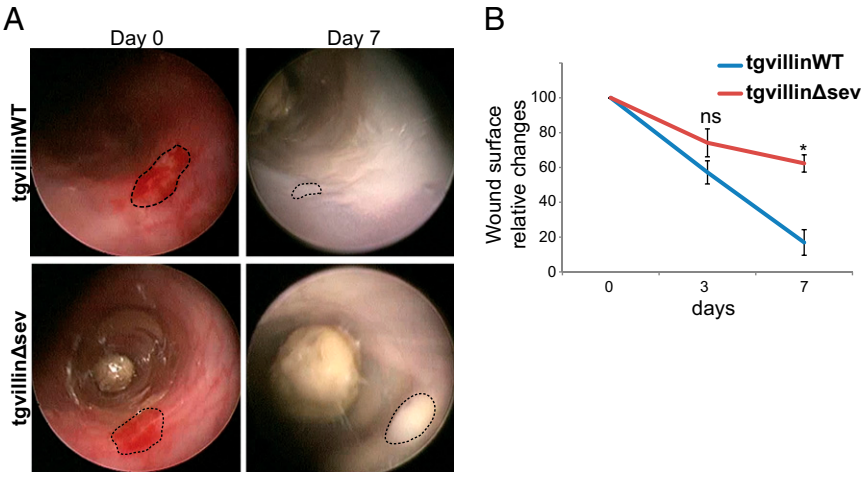

Fig. 3. Efficient colonic wound healing requires villin through its severing activity. (*A*) Serial endoscopic snapshots showing the site of biopsy-induced injury in mouse colon of the indicated genotypes at day 0 and 7 after wounding. Images are representative of at least four animals per genotype. Dashed lines delineate the wounded area. (*B*) Plot of the average changes in the wounded area changes over time for mice of the indicated genotype, normalized to the original lesion size at day 0. Values are for tgvillinWT and tgvillinΔsev, respectively; day 3: 57 ± 6 vs. 74 ± 8%; day 7: 17 ± 8 vs. 62 ± 5%. Number of animals analyzed: WT: $n = 4$; tgvillinΔsev, $n = 5$. *$P < 0.05$. ns, nonsignificant ($P > 0.05$); Wilcoxon.

culture to overcome limitations intrinsic to in vivo systems. We required a cell-culture model that would closely recapitulate the apico-basal polarization and differentiation of enterocytes in vivo. We chose the nontransformed porcine epithelial LLC-PK1 cell line derived from kidney proximal tubules, which classically is used to study microvillus biology and which also expresses villin. We generated a stable cell line expressing an actin-enhanced yellow fluorescent protein (EYFP) construct using a clonal approach, resulting in nearly 100% homogeneity. Depletion of endogenous villin was performed using two separate shRNAs, both of which resulted in a depletion of nearly 80% in confluent cells (Fig. S3*A*). We then chose one shRNA to pursue our experiments and express the mCherry-villin constructs. After transfection, mCherry-villinWT or mCherry-villinΔsev FACS-sorted cells showed comparable expression levels as seen by Western blot, further confirming endogenous villin depletion (Fig. S3*C*). We then characterized the cellular distribution of the transfected proteins and detected an important colocalization of the mCherry-fused proteins and EYFP-actin in the apical microvilli of confluent unwounded LLC-PK1 sorted cells (Fig. S4). In addition, expression of both villin constructs resulted in a similar marked increase in microvillus size compared with nontransfected cells depleted for endogenous villin (Fig. S4). Thus, as previously reported (27), the mCherry-villin proteins retain their correct subcellular localization and their morphogenetic effects in LLC-PK1 cells.

To evaluate the previously reported role of villin during cell migration and to validate our cell-culture system, we used small silicon inserts dedicated to 2D wound-healing assays, allowing robust quantification under different experimental conditions. Time-lapse multiposition microscopy revealed a modest but statistically significant decrease in the relative area colonized by the monolayer of villin-depleted LLC-PK1 cells at 10 h normalized to cells expressing the empty vector (72 ± 5 and 71 ± 5% for shRNA1 and shRNA2, respectively; $P < 0.001$ for each, t test), indicating inefficient migration in the absence of villin (Fig. S3*B*). WT villin re-expression significantly enhanced normalized cell migration (100 ± 4.5 vs. 60 ± 3% for villin-depleted cells re-expressing villinWT and villin depleted cells, respectively; $P < 0.001$, t test), thus, functionally rescuing the depletion of endogenous villin (Fig. S3*D*). In contrast, the migratory properties of cells re-expressing the villin-severing mutant were not significantly different from those of villin-depleted cells (70 ± 5 vs. 60 ± 3%; $P > 0.05$, t test) (Fig. S3*D*). These results confirm that villin improves the efficiency of wound closure in vitro and further demonstrate the importance of its F-actin–severing property.

Villin's Severing Activity Participates in the Microvillus Disassembly Required for Efficient Cell Migration. Most epithelial cells are able to migrate in the absence of villin. Thus, villin must have a specific function in highly differentiated cells with developed microvilli. To obtain further insights at the subcellular level into villin regulation of cell reorganization during migration, we analyzed the wound-healing process by time-lapse imaging using high-resolution spinning-disk confocal microscopy. Cell migration was induced by scratch assays of cell monolayers of the previously described cell lines. In agreement with past results (22), lamellipodia displayed a marked concentration of mCherry-villin, which overlapped with the narrow intense actin-EYFP signal. Villin devoid of its F-actin–severing property also showed lamellipodial recruitment. In cells re-expressing WT mCherry-villin, major apical pole remodeling was consistently observed, concomitantly with lamellipodial extension. Indeed, a rapid disassembly of EYFP-actin– and mCherry-villinWT–positive microvilli could be observed on the x,y plane of the migrating cells and was confirmed by x,z reconstruction (Fig. 4 *A* and *B*). The x,z representation also allowed us to quantify the relative apical fluorescence intensities during cell migration. Accordingly, we noticed a rapid conspicuous decrease in the relative intensities of actin and villin apical fluorescence (Fig. 4*C*). Thus, microvilli are disassembled rapidly upon cell migration in the presence of villin. In contrast, in most of the migrating villinΔsev-positive LLC-PK1 cells, the apical microvilli were stable and showed no apparent disassembly (Fig. 4 *A* and *B*). Consequently, the decrease in the relative intensity of apical fluorescence was significantly lower than in the previous condition (Fig. 4*C*). To confirm this phenotype, the presence or absence of apical microvilli revealed by the mCherry-villin proteins was quantified on cells fixed at 30 min after wounding. A majority of migrating cells re-expressing WT villin were devoid of microvilli whereas this number was significantly reduced in cells expressing villinΔsev (62.5 vs. 43.4% for villinWT and villinΔsev, respectively; $P < 0.001$) (Fig. 4*D*). Together, these results clearly demonstrate that villin is required to sever microvillar actin filaments efficiently, resulting in disassembly of the brush border at the onset of cell migration.

Microvillar Actin Is Integrated Rapidly at the Lamellipodia upon Migration. The enhancement of epithelial cell migration induced by villin's severing activity correlates with the disassembly of apical microvilli. Therefore, it is possible that the lack of apical pole disassembly in the severing mutant may hinder the repolarization of the cells toward a migratory phenotype. In agreement with this idea, a precise quantification of the scratch wound assays demonstrated a significant decrease in the rate of lamellipodia formation in villinΔsev-expressing cells compared

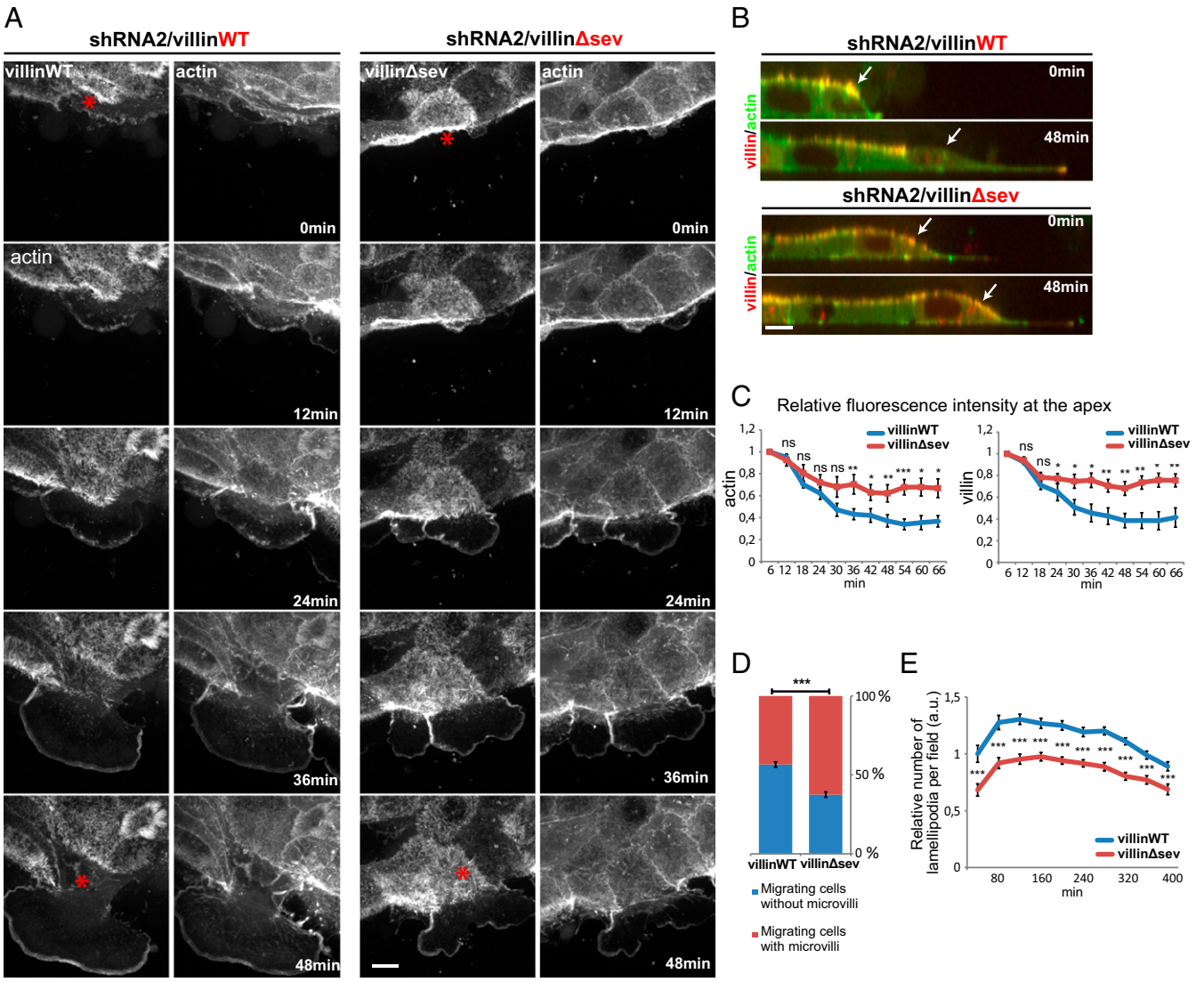

Fig. 4. Microvilli disassemble upon cell migration via villin's severing activity. (*A*) Migration of LLCPK-1 cells depleted for endogenous porcine villin (shRNA2) expressing EYFP-actin and mCherry-villinWT or villinΔsev visualized by spinning-disk time-lapse microscopy. EYFP and mCherry channels are shown. Images are maximal projections of the acquired z stacks. Serial images are shown at 12-min intervals. Red asterisks indicate the migrating cells analyzed. (Scale bar: 10 μm.) (*B*) Z reconstructions of the migrating cells highlighted in *A* at 0 and 48 min. Overlays of EYFP-actin (green) and mCherry-villin (red) are shown. White arrows point to the dorsal face of the migrating cell. (Scale bar: 10 μm.) (*C*) Plots depicting the intensity of villin and actin fluorescence over time at the dorsal face of the cells transfected for mCherry-villinWT or villinΔsev quantified from images acquired by spinning-disk time-lapse microscopy. Number of cells analyzed: villinWT, n =10; villinΔsev, n =19. (*D*) Histogram representing the penetrance of the phenotype illustrated by the presence or absence of apical microvilli positive for mCherry-villin on migrating cells transfected for mCherry-villinWT or villinΔsev at 30 min postinjury on fixed cells. Values are 62.5 ± 1.7 and 43.4 ± 1.7% for villinWT and villinΔsev, respectively. ***$P < 0.001$, t test. Number of cells analyzed: villinWT, n =121; villinΔsev, n = 95. (*E*) Relative number of lamellipodia formation per field over time in villinWT- or villinΔsev-expressing cells. Values are normalized to the number of lamellipodia at 20 min postinjury determined in villinWT-expressing cells. Values are averaged from three experiments.

with villinWT cells at the onset of migration (Fig. 4*E*). We next questioned whether the microvillar actin was required for lamellipodia formation by being recruited directly and rapidly into migratory structures. We followed the intracellular dynamics of microvillar actin in migrating cells using a photoactivatable GFP (PAGFP)-actin construct (31), in confluent LLC-PK1 cells depleted for endogenous villin and expressing either villinWT or villinΔsev. Actin molecules were locally photoactivated specifically at the apex of leading LLC-PK1 cells (Fig. 5*A*) after monolayer scratching. A rapid and consequent recruitment of PAGFP-actin could be observed at the lamellipodium of cells expressing WT villin (Fig. 5*B*). In contrast, the recruitment of photoactivated PAGFP molecules was strongly decreased in cells expressing villinΔsev (Fig. 5*B*). Accordingly, quantifications of the ratio of photoactivated actin molecules recruited to the lamellipodia revealed a prompt redistribution of microvillar actin toward the lamellipodia of cells expressing WT villin, whereas recruitment was significantly reduced in cells expressing villinΔsev (17 ± 7 vs. 4 ± 0.8% at 6 min after photoactivation; $P < 0.05$, t test) (Fig. 5*C*). To exclude a bias caused by a possible difference in the actin exchange and/or assembly at the lamellipodium of cells expressing villinWT or villinΔsev, we photoactivated PAGFP-actin molecules in the lamellum, in a region positioned slightly away from the lamellipodial leading edge, and monitored integration at the lamellipodium. Importantly, quantifications did not show that villin severing of F-actin influenced the rate of lamellar actin integration at the lamellipodium (Fig. 5*D*). Because of the fast actin treadmilling in microvilli (32, 33),

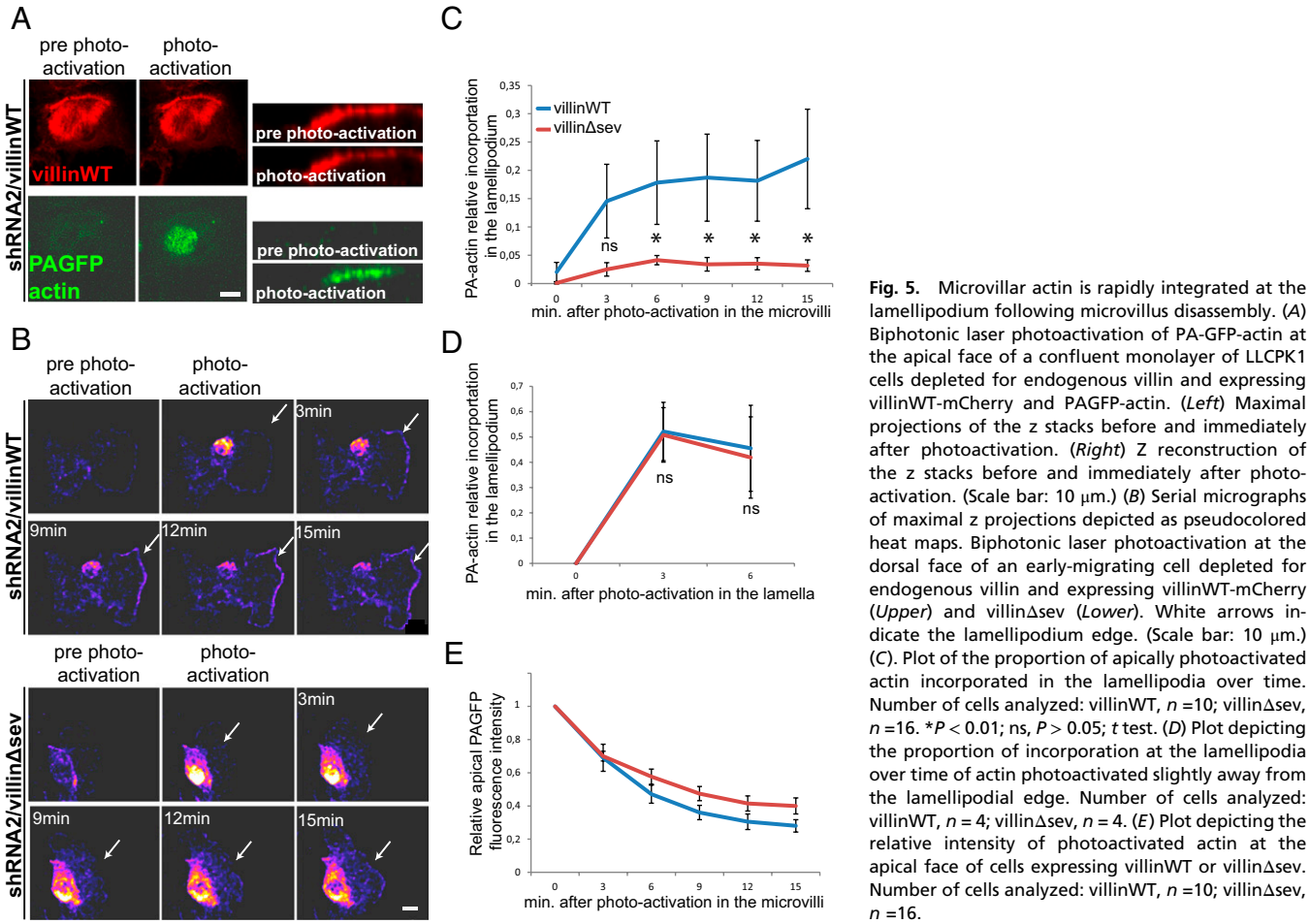

Fig. 5. Microvillar actin is rapidly integrated at the lamellipodium following microvillus disassembly. (*A*) Biphotonic laser photoactivation of PA-GFP-actin at the apical face of a confluent monolayer of LLCPK1 cells depleted for endogenous villin and expressing villinWT-mCherry and PAGFP-actin. (*Left*) Maximal projections of the z stacks before and immediately after photoactivation. (*Right*) Z reconstruction of the z stacks before and immediately after photoactivation. (Scale bar: 10 μm.) (*B*) Serial micrographs of maximal z projections depicted as pseudocolored heat maps. Biphotonic laser photoactivation at the dorsal face of an early-migrating cell depleted for endogenous villin and expressing villinWT-mCherry (*Upper*) and villinΔsev (*Lower*). White arrows indicate the lamellipodium edge. (Scale bar: 10 μm.) (*C*). Plot of the proportion of apically photoactivated actin incorporated in the lamellipodia over time. Number of cells analyzed: villinWT, n =10; villinΔsev, n =16. *$P < 0.01$; ns, $P > 0.05$; t test. (*D*) Plot depicting the proportion of incorporation at the lamellipodia over time of actin photoactivated slightly away from the lamellipodial edge. Number of cells analyzed: villinWT, n = 4; villinΔsev, n = 4. (*E*) Plot depicting the relative intensity of photoactivated actin at the apical face of cells expressing villinWT or villinΔsev. Number of cells analyzed: villinWT, n =10; villinΔsev, n =16.

the PAGFP-actin is not expected to remain stable at the apex of the cells even in the absence of villin's severing activity. We nevertheless could detect a slight but not significant increase in PAGFP-actin stability in cells expressing villinΔsev (Fig. 5*E*). Thus, these results show that actin molecules resulting from microvillus disassembly mediated by villin's F-actin–severing property are integrated rapidly at the nascent lamellipodium, without modification of the lamellipodium actin polymerization rate.

Villin Is Essential for Microvillus Disassembly upon Cell Migration in Vivo. Using a wound-healing model in cell culture, we could describe dynamically and quantify an important apical domain remodeling induced by villin's severing property at the onset of cell migration. To assess the relevance of this newly demonstrated function of villin in a more physiological situation, we wondered whether similar rapid cell reorganization occurs during intestinal wound healing in vivo. However, the extent of the biopsy-induced injury (Figs. 1 and 3) and the subsequent time scale of the healing process prevented the use of this technique to evaluate such prompt and precise cell response. Instead we chose to induce more accurate chemical lesions by the bile acid sodium deoxycholate (DOC), which produces sharp lesions restricted to the epithelial cells on the upper part of the intestinal villi (34, 35), as observed on histological paraffin sections of the injured tissue (Fig. 6*A*, *Upper*). E-cadherin immunostaining, which delineates basolateral boundaries of the cells, revealed that the enterocytes immediately adjacent to the wound conserved a columnar shape. These cells also retained the exclusion of E-cadherin from the apical domain, as expected for a polarized epithelium. Importantly, the digestive enzyme sucrase-isomaltase maintained a strict apical subcellular distribution on these cells. Thus, apico-basal polarity is preserved on the enterocytes immediately after injury to adjacent cells. Bile acid-induced injuries were similar on the epithelia of WT and villin-null mice (Fig. 6*A*, *Upper*). Subsequently, DOC was washed out to allow epithelium restitution. After 30 min, dramatic cell reorganization of the enterocytes adjacent to the wound could be detected in WT mice, revealing a progressive flattening of the epithelial cells as seen with the E-cadherin staining (Fig. 6*A*, *Lower*). E-cadherin was no longer excluded from the apex, suggesting an alteration of apico-basal polarity (Fig. 6*A*, *Lower*) and microvillus disassembly as confirmed by the loss of the intense apical phalloidin staining of the brush border in WT cells close to the wounded area (Fig. S5*A*). In contrast, in villin-null mice, most of the cells in contact with the injury conserved an intense sucrase-isomaltase apical staining, indicating that the efficiency of microvillus disassembly was strongly impaired (Fig. 6*A*). To quantify this phenotype, the proportion of cells at the wound margin bearing apical sucrase-isomaltase and ezrin, two microvillus markers, was evaluated in WT, villin-null, tgvillinWT, and tgvillinΔsev mice after DOC injury. Strikingly, most of the WT and tgvillinWT cells had lost their apical localization of sucrase-isomaltase (77 ± 1 and 79 ± 2%, respectively) and ezrin (75 ± 2 and 73 ± 3%, respectively), indicating extensive microvillus disassembly (Fig. 6 *A* and *B*). In contrast, in villin-null and tgvillinΔsev mice, only a few cells in contact with the injury had lost the intense apical staining for sucrase-isomaltase (27 ± 4 and 21 ± 3%, respectively) and ezrin (16 ± 4 and 28 ± 3%, respectively), indicating that the efficiency of microvillus disassembly was strongly impaired (Fig. 6 *A* and *B*). These in vivo observations

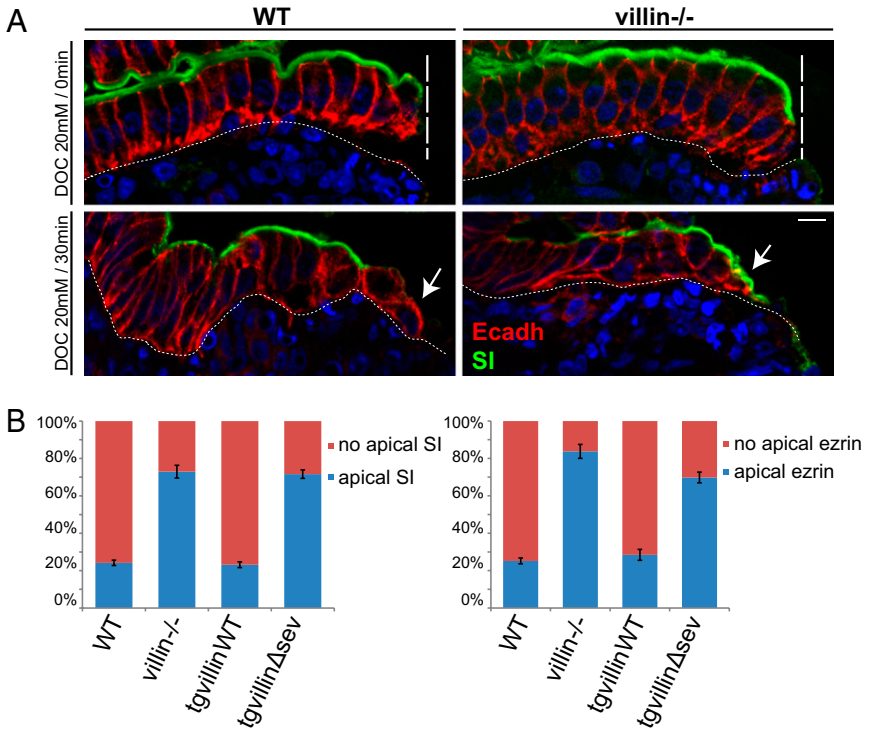

Fig. 6. Villin is essential for brush border disassembly upon cell migration in vivo. (*A*) Histological paraffin sections of small intestine of WT or villin$^{-/-}$ mice luminally treated with DOC just after washout (*Upper*) or 30 min after washout (*Lower*) stained for E-cadherin (Ecadh, red) and sucrase-isomaltase (SI, green). DAPI labels nuclei (blue). Vertical dashed lines highlight the injured area; basal dashed lines delineate the lamina propria; arrows indicate the injury-adjacent enterocytes. (Scale bar: 10 μm.) (*B*) Histograms depicting the presence or the absence of apical staining of sucrase-isomaltase or ezrin quantified 30 min after washout on histological paraffin sections of small intestine of WT, villin$^{-/-}$, tgvillinWT, or tgvillinΔsev mice treated with DOC. Values are WT, 23 ± 1%; villin$^{-/-}$, 77 ± 4%; tgvillinWT, 21 ± 2%; and tgvillinΔsev, 79 ± 3% for apical sucrase-isomaltase and WT, 25 ± 2%; villin$^{-/-}$; 84 ± 4%; tgvillinWT, 27 ± 3%; and tgvillinΔsev, 72 ± 3% for apical ezrin. For sucrase-isomaltase: WT, n = 84 cells analyzed from eight animals; villin$^{-/-}$, n = 147 cells analyzed from 12 animals; tgvillinWT, n = 29 cells analyzed from three animals; tgvillinΔsev, n = 41 cells analyzed from three animals. For ezrin: WT, n = 45 cells analyzed from six animals; vil$^{-/-}$, n = 26 cells analyzed from three animals; tgvillinWT, n = 22 cells analyzed from three animals; tgvillinΔsev, n = 35 cells analyzed from three animals.

fully corroborate the cell remodeling reported upon cell migration in culture (Fig. 4). To exclude the possibility that the observed cell reorganizations are caused by an eventual apoptotic program, we performed cleaved caspase 3 staining and detected very few apoptotic enterocytes adjacent to the wound, independently of the two genotypes (Fig. S5 *B* and *C*). Thus, we can conclude that villin is essential for the disassembly of microvilli and for apical-domain remodeling elicited by wound healing in vivo, via its actin-severing property.

Discussion

In this study we definitively demonstrate that villin, a microvillar actin-binding protein, participates directly in apical pole remodeling of migrating cells and promotes colonic and intestinal epithelial wound closure in vivo. We show that villin severs F-actin within microvilli to initiate their disassembly at the onset of cell migration. We provide direct evidence that villin-mediated severing of F-actin induces the rapid integration of microvillar actin into lamellipodia and stimulates cellular motility. We demonstrate the physiological and biological function of villin in microvillus-expressing cells such as the enterocytes of the gut, an organ subject to injuries that would be deleterious without a rapid and effective mucosal healing process.

Villin Plays a Direct Role in Promoting Enterocyte Migration upon Wound Healing. Past studies have described a protective role for villin during tissue injury in the mouse colon, although divergent hypotheses have been drawn (20, 21). In fact, the experimental procedure that was applied precluded determining whether villin influences the extent of tissue injury or instead the process of tissue repair. To circumvent potential cell homeostatic responses to chemical methods of injury, we produced localized instantaneous mechanical lesions of the mouse colonic mucosa. Temporal observation of the original injury by endoscopy allowed a robust quantification of tissue recovery and confirmed rapid healing in presence of villin. Importantly, using this mechanical method, we could not detect any differences in cell survival or proliferation caused by the absence of villin and so could exclude a role for these processes. In cooperation with proliferation, cell migration plays a major role during wound healing in the digestive tract as well as in other organs (2, 4, 28, 36). Ectopic expression of villin has been shown to increase the migration efficiency of several epithelial cell lines. The careful in vivo analyses reported here definitely prove that migratory defects indeed are responsible for the inefficient gut wound repair in the absence of villin, independently of its antiapoptotic function.

Villin-Severing Activity Is Responsible for Improved Epithelial Restitution. Using a single-copy, targeted insertion transgenic approach, we were able to express in villin-knockout mice a specific severing mutant of villin and, as a control, its WT version which completely rescued the knockout phenotype. Mechanical wounding experiments performed on these mouse models proved that villin function in mucosal healing relies entirely on its severing property. Villin's severing activity has previously been shown to enhance actin-based motility of functionalized beads in vitro and of bacteria in infected cells (26). In this report, we show that the loss of villin's severing activity also results in inefficient migration of epithelial cell monolayers by performing wound-healing assays on polarized LLC-PK1 cells depleted for endogenous villin or re-expressing the villin severing mutant. How is villin's severing activity activated in migrating cells? Following injury, an immediate elevation of intracellular Ca^{2+} in wound-adjacent cells has been reported in several systems in vitro and in vivo (37, 38). In addition, the regulation of cell migration by villin appears to require its phosphorylation (22, 23). Interestingly, both elevated calcium and phosphorylation of villin activate its severing activity (16, 19, 39, 40). Thus, biochemical signaling pathways associated with wound responses and cell migration likely are able to regulate villin's severing property. How then does villin's severing activity regulate cell motility? Villin localizes to the lamellipodium and favors its protrusion, as shown in this study, presumably by enhancing actin dynamics as inferred from in vitro actin-based motility assays (22, 26). Thus, villin could directly influence the motility machinery of epithelial cells. Although we

could not detect an increase in lamellipodial actin dynamics in the presence of villin, the severing activity of villin may participate indirectly in cell movement by mobilizing actin monomers stored as filaments in other subcellular structures.

Villin's Severing Activity Induces Microvillus Disassembly and Enterocyte Depolarization. We provide dynamic proof of sudden microvillus disassembly, demonstrated by the loss of structural and functional proteins, at the onset of cell migration in LLC-PK1 cells. Of high importance, we were able to confirm that the aforementioned apical remodeling occurs similarly in vivo. Our results in vivo and in cell culture furthermore demonstrate that villin's severing of F-actin is required to induce such apical pole remodeling. In fact, we report that the phenotype is substantially stronger in vivo than in LLC-PK1 cells, probably because of the difference between a complete knockout of the villin gene in mice compared with a knockdown in LLC-PK1 cells. Other actin-depolymerizing proteins such as actin depolymerizing factor (ADF)/cofilin have been proposed to participate in the disassembly of microvilli from kidney proximal tubules following ischemia/reperfusion stress in vivo (41, 42). ADF/cofilin, however, is not present in the brush border of intact kidney or intestinal epithelial cells (42–44). ADF/cofilin could act in concert with villin, but only as a second step, after the initiation of the process by the microvillus-resident villin. Thus, our results and these past observations strongly argue that initial intestinal microvillus disassembly is triggered by villin's severing of microvillar actin filaments. Therefore, villin is a direct molecular effector of enterocyte apical pole remodeling in vivo in a migratory context. Moreover, the impairment of microvillus disassembly in the presence of a villin affected in its severing property is associated with a reduction in the number of cells developing lamellipodia, i.e., cells that have efficiently repolarized toward a migratory organization. Thus, enterocytes require severing of microvillus F-actin by villin to initiate their repolarization efficiently.

Microvillus Disassembly and Efficient Enterocyte Migration. Apical pole reorganization is not specific to migrating intestinal epithelial cells (45–47). Rather, it occurs widely in different organs and seems intrinsic to the migratory phenotype of polarized epithelial cells that undergo extensive reorganization to become motile without perturbing the integrity of the monolayer (48). Why would apical pole depolarization be important for enterocyte migration? Several biological and biophysical points can be raised. First, the precise regulation of plasma membrane tension is critical for efficient migration. Indeed, artificially increasing the membrane tension impairs the efficiency of lamellipodial migration (49). On polarized epithelial cells, membrane tension is higher on the apical than on the basolateral pole (50). This discrepancy is caused by the domains of distinct lipid composition generated by the physical separation of tight junctions and likely is reinforced further by the presence of numerous membrane protrusions: the microvilli (51, 52). Their disassembly may alleviate membrane tension and thereby favor migration. Second, microvilli use important quantities of diverse cellular components. For instance, apical microvilli occupy a great amount of plasma membrane. Rapid cell-surface changes such as lamellipodial protrusions require net membrane addition, because plasma membrane is basically inextensible (53). We can speculate that the disassembly of microvilli releases important quantities of plasma membrane, in a manner similar to that recently described for caveolae (54). Analogously, microvilli concentrate high amounts of actin. We estimated that the brush border concentrates more than 50% of the total phalloidin signal in the mouse enterocyte ($52 \pm 5\%$; $n = 6$). Its disruption would release numerous short filaments that would depolymerize and increase the availability of free actin monomers (55). In support of this idea, we observed, following microvillus disassembly, prompt recruitment of microvillar actin to the lamellipodium of cells expressing villin. Conversely, the recruitment was reduced and slower in cells expressing the villin mutant affected in actin severing. Therefore, it is likely that villin stimulates cell migration indirectly by supplying actin monomers. Indeed, two published observations argue in favor of this scenario. The cytoplasmic concentration of actin monomers largely determines the magnitude of lamellipodial extension (56). Furthermore, ADF/cofilin can support lamellipodial extension indirectly by supplying an abundant pool of actin monomers (57). Thus, villin probably has a comparable impact on lamellipodial dynamics and cell migration. However, its specific localization and regulated activation restrict its function to a highly specialized domain, the apical microvilli, where it is the only described severing protein, and to situations of stress.

In conclusion, this work illustrates the importance of the disassembly of highly specialized apical poles for the effective repolarization of epithelial cells initiating migration upon injury. It shows how enterocytes have developed specific molecular machinery, based on the severing of actin filaments by villin, to provoke a rapid and efficient disassembly of microvilli and to stimulate cell migration. This work highlights the importance of direct cytoskeletal effectors that mediate the loss of apico-basal polarity during wound healing.

Materials and Methods

Mice Generation. Villin-mCherry constructs (WT or Δsev) were inserted in a pENTRY vector (Addgene) previously modified to include the ubiquitous cytomegalovirus immediate-early enhancer CAG promoter driving a lox-chloramphenicol acetyltransferase-lox construct. The transgene then was transferred by the Gateway technology into a destination vector pDEST-HPRT (Nucleis) carrying two homologous arms of the *HPRT* gene. Transgenic animals carrying a single copy of one or the other transgenes inserted at the *HPRT* locus were obtained using the Speedy Mouse technology (58). Resulting chimeric males were bred with C57BL/6 females, and the F1 agouti off-springs were backcrossed with C57BL/6 animals. Plasmid recombination was induced by chronic tamoxifen injections. Briefly, mice, including controls, were injected i.p. with tamoxifen (50 μg/g of animal body weight) on 2 consecutive d/wk for a total of 4 wk.

Image Analysis. All images were processed and pseudocolored using ImageJ (National Institutes of Health). Measurements and analyses were performed using the same software. Images comparing different genotypes or experimental conditions were acquired and postprocessed with identical parameters.

Sampling and Preparation of the Tissues for Histological Analyses. Short pieces of intestinal or colonic samples were washed with PBS. To prepare tissue for paraffin sectioning, tissues were fixed in 4% paraformaldehyde or in Carnoy solution (60% ethanol, 30% chloroform, and 10% acetic acid) for 2 h at room temperature or overnight at 4 °C. The samples then were ethanol dehydrated and embedded in paraffin. For frozen sections, tissues were fixed for 2 h in PFA 4% and incubated overnight in a 30% glucose solution diluted in PBS or were snap frozen in 2-methylbutane precooled by liquid nitrogen. They then were embedded in optimal cutting temperature medium (OCT) and frozen at −80 °C.

Immunohistochemistry. Histological sections of 5 or 8 μm were prepared from paraffin- or OCT-embedded tissues, depending on the experiment. Paraffin was removed from paraffin sections using xylene. Sections then were hydrated with ethanol solutions of decreasing concentrations. The epitopes were unmasked by boiling for 20 min in Antigen Unmasking Solution (Vector Laboratories). For frozen sections, OCT was removed by PBS washes. OCT-embedded snap-frozen tissues were postfixed in 4% PFA for 20 min. Sections were incubated for 45 min at room temperature in blocking buffer (3% FCS in PBS) and then overnight at 4 °C with primary antibody (Table S1) diluted in 3% FCS. After several washes, secondary fluorescent antibody was added for 90 min. For some experiments, Alexa Fluor 488 phalloidin was used (Life Technologies). Representative images from immunostaining were acquired using an Apotome system with a 10× or 63× water Plan-Apochromat lens (Carl Zeiss) or CM60 epifluorescence microscope (Leica) or an inverted confocal spinning-disk Eclipse Ti Roper/Nikon microscope, all coupled to a Coolsnap HQ2 camera (Photometrics).

In Vivo Experiments. Animal experiments were carried out under the authority of the Curie Institute veterinarian, under permission granted to the Robine laboratory (number 75–433, Préfecture de Police - Direction des Services Vétérinaires de Paris). Experiments in transgenic mice were carried out on sex-matched mice of similar age. For living-animal experiments, anesthesia was performed by injection of a ketamine/xylazine mix (100 mg/mL each) diluted in 150 mM NaCl. Mice were killed at the end of experiments by cervical dislocation.

Carbachol Treatment. After mouse anesthesia, a jejunum loop was isolated in situ, taking care not to injure the local vasculature. The loop was placed carefully in a Petri dish containing 10 μM carbachol (Sigma Chemical Co.) solution diluted in PBS plus Ca^{2+} (10 mM) for 20 min to achieve a basolateral infusion of the drug. After mice were killed, small samples of treated tissue were washed and snap frozen in precooled 2-methylbutane. The experiment was repeated in at least three different animals per genotype. For a more detailed protocol, see ref. 20.

Procedure for Biopsy-Induced Injury and Mouse Endoscopy. A straight-type rigid miniature endoscope Coloview mouse endoscopic system (Karl-Storz) linked to an Archos 48 tablet (Archos) for video acquisition was used to visualize mouse colon. After mouse anesthesia, the endoscope probe was introduced to the mid-descending colon. Then a flexible 3-French biopsy forceps was inserted and was used to remove an area of the entire mucosa and submucosa, avoiding penetration of the muscularis propria. Particular care was taken to generate lesions of comparable size. Tissue healing was monitored by endoscopy at days 3 and 7 postinjury. The tissue-healing process was quantified by measuring the wounded area using ImageJ on extracted images. The images were chosen carefully to show similar viewpoints in terms of endoscopy camera orientation and distance from the injury. For tissue analysis, the injured area was localized with the endoscopic probe on killed mice. The corresponding colon segment then was sampled and processed for immunohistochemistry. The number of mice analyzed is stated in the figure legends.

Bile Salt-Induced Injuries. After mouse anesthesia, a small incision was made to allow access to the small intestine. Two knots were made using surgical suture thread to isolate a small intestinal segment. Particular caution was taken to avoid any damage to local vasculature. The intestinal loop then was filled with a DOC solution diluted in PBS at 20 mM for 5 min. After several washes with PBS, the segment was filled with DMEM supplemented with 20% FCS. Suture thread then was removed. The intestinal loop was replaced carefully inside the mouse, and cell restitution was allowed for 30 min. Then the treated tissue was washed vigorously in PBS, fixed in Carnoy solution, and subsequently processed for immunohistochemistry. The number of mice analyzed is stated in the figure legends.

Cell Culture and Transfection. LLC-PK1 cells (CCL 101; American Type Culture Collection) were given by M. Arpin (UMR144, Institut Curie, Paris), and grown in DMEM (Invitrogen) containing 10% (vol/vol) FCS. LLC-PK1 cells were transiently transfected by electroporation. The stable LLC-PK1 cell line expressing actin-EYFP was obtained through a clonal approach using cloning rings after selection by G418 (Invitrogen). This cell line subsequently was used to obtain cell lines depleted for endogenous villin and enriched in mCherry-villinWT– or mCherry-villinΔsev–expressing cells by fluorescence-activated cytometry cell sorting (FacsVantage Diva; BD Biosciences). Lentiviral particles were obtained by transfection of HEK293T cells with lentiviral vector in addition to plasmids encoding vesicular stomatitis Indiana virus (pVSVG) and grouped antigens (pGAG) by Polyethylenimine (PolyPlus) in a biosafety level 3 compliant laboratory. Medium containing viral particles was collected 48 h after transfection and were filtrated using 0.44 μm sterile filters. Then 1 mL of medium containing viral particles was added to 25×10^4 LLC-PK1 cells seeded in six-well plates. Twenty-four hours after infection cells were vigorously washed and selected using Puromycin (Life Technologies). G418 was used at 500 μg/mL. Puromycin was used at 1 μg/mL.

Photoactivation Experiments. LLC-PK1 cells depleted for endogenous villin (shRNA2) were cotransfected with PA-GFP-actin and mCherry-villinWT or mCherry-villinΔsev plasmids. After cell recovery, they were seeded at confluence (1×10^6 cells) in glass-bottomed dishes and were grown overnight. The scratching assay then was performed as described earlier. Experiments were carried out using the 40×/1,3 OIL DICII PL APO objective of an inverted Laser Scanning Confocal LSM710NLO (Carl Zeiss) coupled with a Mai Tai biphotonic laser (Spectra Physics-Newport Corp). Using the ZEN software (Carl Zeiss), we selected a small region in the dorsal face of the cell. Caution was taken to select regions of similar size in the different cells analyzed. A laser single pulse at 810-nm wavelength (2×405 nm) was burst in the region of interest to photoactivate PA-GFP. Time-lapse acquisition was performed using the confocal mode with stacks of 1-μm z interval. Images stacks were denoised identically (59).

ACKNOWLEDGMENTS. We thank initially Frédéric Jaisser and then Noura Mebirouk, Christophe Alberti, and Elodie Belloir for helping in the generation of mouse models; Shannon Duffy, Klaus-Peter Janssen, Maia Chanrion, Silvia Fre, Sara Geraldo, François Xavier Gobert, and Maria Teresa Maia for advice and careful reading of the manuscript; Stéphanie Boissel and all members of the animal house facility, the FACS facility, and the Platform for Cell and Tissue Imaging of the Curie Institute (PICT-IBISA); the Nikon Imaging Centre at the Curie Institute, particularly O. Renaud and O. Leroy; and Virginie Dangles-Marie and Isabelle Grandjean for the animal house management. The Curie Institute Foundation funded this work. F.U. was supported by the Ministère de la Recherche et de la Technologie and the Fondation pour la Recherche Médicale (FRM). This work also was supported by grants from the FRM (to M.C.) and the European Union grant, Fond Européen de Développement Régional (FEDER) (to M.C.), in part by federal funds from the US Department of Agriculture, Agricultural Research Service, under Cooperative Agreement no. 58-6250-1-003, and also by Public Health Service grant DK56338, which funds the Texas Medical Center Digestive Diseases.

1. Blikslager AT, Moeser AJ, Gookin JL, Jones SL, Odle J (2007) Restoration of barrier function in injured intestinal mucosa. *Physiol Rev* 87(2):545–564.
2. Sturm A, Dignass AU (2008) Epithelial restitution and wound healing in inflammatory bowel disease. *World J Gastroenterol* 14(3):348–353.
3. Iizuka M, Konno S (2011) Wound healing of intestinal epithelial cells. *World J Gastroenterol* 17(17):2161–2171.
4. Lotz MM, Rabinovitz I, Mercurio AM (2000) Intestinal restitution: Progression of actin cytoskeleton rearrangements and integrin function in a model of epithelial wound healing. *Am J Pathol* 156(3):985–996.
5. Fenteany G, Janmey PA, Stossel TP (2000) Signaling pathways and cell mechanics involved in wound closure by epithelial cell sheets. *Curr Biol* 10(14):831–838.
6. Nusrat A, Delp C, Madara JL (1992) Intestinal epithelial restitution. Characterization of a cell culture model and mapping of cytoskeletal elements in migrating cells. *J Clin Invest* 89(5):1501–1511.
7. Louvard D, Kedinger M, Hauri HP (1992) The differentiating intestinal epithelial cell: Establishment and maintenance of functions through interactions between cellular structures. *Annu Rev Cell Biol* 8:157–195.
8. Miyoshi J, Takai Y (2008) Structural and functional associations of apical junctions with cytoskeleton. *Biochim Biophys Acta* 1778(3):670–691.
9. Rottner K, Stradal TEB (2011) Actin dynamics and turnover in cell motility. *Curr Opin Cell Biol* 23(5):569–578.
10. Dignass A, Lynch-Devaney K, Kindon H, Thim L, Podolsky DK (1994) Trefoil peptides promote epithelial migration through a transforming growth factor beta-independent pathway. *J Clin Invest* 94(1):376–383.
11. Mashimo H, Wu DC, Podolsky DK, Fishman MC (1996) Impaired defense of intestinal mucosa in mice lacking intestinal trefoil factor. *Science* 274(5285):262–265.
12. Santos MF, et al. (1997) Rho proteins play a critical role in cell migration during the early phase of mucosal restitution. *J Clin Invest* 100(1):216–225.
13. Cetin S, et al. (2004) Endotoxin inhibits intestinal epithelial restitution through activation of Rho-GTPase and increased focal adhesions. *J Biol Chem* 279(23):24592–24600.
14. Rao JN, et al. (2008) Rac1 promotes intestinal epithelial restitution by increasing Ca2+ influx through interaction with phospholipase C-(gamma)1 after wounding. *Am J Physiol Cell Physiol* 295(6):C1499–C1509.
15. Xu LF, et al. (2011) Disruption of the F-actin cytoskeleton and monolayer barrier integrity induced by PAF and the protective effect of ITF on intestinal epithelium. *Arch Pharm Res* 34(2):245–251.
16. Bretscher A, Weber K (1980) Villin is a major protein of the microvillus cytoskeleton which binds both G and F actin in a calcium-dependent manner. *Cell* 20(3):839–847.
17. Glenney JR, Jr., Geisler N, Kaulfus P, Weber K (1981) Demonstration of at least two different actin-binding sites in villin, a calcium-regulated modulator of F-actin organization. *J Biol Chem* 256(15):8156–8161.
18. Glenney JR, Jr., Kaulfus P, Weber K (1981) F actin assembly modulated by villin: Ca++-dependent nucleation and capping of the barbed end. *Cell* 24(2):471–480.
19. Zhai L, et al. (2002) Regulation of actin dynamics by tyrosine phosphorylation: Identification of tyrosine phosphorylation sites within the actin-severing domain of villin. *Biochemistry* 41(39):11750–11760.
20. Ferrary E, et al. (1999) In vivo, villin is required for Ca(2+)-dependent F-actin disruption in intestinal brush borders. *J Cell Biol* 146(4):819–830.
21. Wang Y, et al. (2008) A novel role for villin in intestinal epithelial cell survival and homeostasis. *J Biol Chem* 283(14):9454–9464.
22. Athman R, Louvard D, Robine S (2003) Villin enhances hepatocyte growth factor-induced actin cytoskeleton remodeling in epithelial cells. *Mol Biol Cell* 14(11): 4641–4653.

23. Tomar A, et al. (2004) Regulation of cell motility by tyrosine phosphorylated villin. *Mol Biol Cell* 15(11):4807–4817.
24. Wang Y, Tomar A, George SP, Khurana S (2007) Obligatory role for phospholipase C-gamma(1) in villin-induced epithelial cell migration. *Am J Physiol Cell Physiol* 292(5):C1775–C1786.
25. Mathew S, et al. (2008) Potential molecular mechanism for c-Src kinase-mediated regulation of intestinal cell migration. *J Biol Chem* 283(33):22709–22722.
26. Revenu C, et al. (2007) Villin severing activity enhances actin-based motility in vivo. *Mol Biol Cell* 18(3):827–838.
27. Pickert G, et al. (2009) STAT3 links IL-22 signaling in intestinal epithelial cells to mucosal wound healing. *J Exp Med* 206(7):1465–1472.
28. Seno H, et al. (2009) Efficient colonic mucosal wound repair requires Trem2 signaling. *Proc Natl Acad Sci USA* 106(1):256–261.
29. el Marjou F, et al. (2004) Tissue-specific and inducible Cre-mediated recombination in the gut epithelium. *Genesis* 39(3):186–193.
30. Robine S, et al. (1985) Can villin be used to identify malignant and undifferentiated normal digestive epithelial cells? *Proc Natl Acad Sci USA* 82(24):8488–8492.
31. Patterson GH, Lippincott-Schwartz J (2002) A photoactivatable GFP for selective photolabeling of proteins and cells. *Science* 297(5588):1873–1877.
32. Tyska MJ, Mooseker MS (2002) MYO1A (brush border myosin I) dynamics in the brush border of LLC-PK1-CL4 cells. *Biophys J* 82(4):1869–1883.
33. Waharte F, Brown CM, Coscoy S, Coudrier E, Amblard F (2005) A two-photon FRAP analysis of the cytoskeleton dynamics in the microvilli of intestinal cells. *Biophys J* 88(2):1467–1478.
34. Moore R, Carlson S, Madara JL (1989) Rapid barrier restitution in an in vitro model of intestinal epithelial injury. *Lab Invest* 60(2):237–244.
35. Masuda K, et al. (2003) Diversity of restitution after deoxycholic acid-induced small intestinal mucosal injury in the rat. *Dig Dis Sci* 48(10):2108–2115.
36. Normand S, et al. (2011) Nod-like receptor pyrin domain-containing protein 6 (NLRP6) controls epithelial self-renewal and colorectal carcinogenesis upon injury. *Proc Natl Acad Sci USA* 108(23):9601–9606.
37. Klepeis VE, Cornell-Bell A, Trinkaus-Randall V (2001) Growth factors but not gap junctions play a role in injury-induced Ca2+ waves in epithelial cells. *J Cell Sci* 114(Pt 23):4185–4195.
38. Sieger D, Moritz C, Ziegenhals T, Prykhozhij S, Peri F (2012) Long-range Ca2+ waves transmit brain-damage signals to microglia. *Dev Cell* 22(6):1138–1148.
39. Glenney JR, Jr., Bretscher A, Weber K (1980) Calcium control of the intestinal microvillus cytoskeleton: Its implications for the regulation of microfilament organizations. *Proc Natl Acad Sci USA* 77(11):6458–6462.
40. Glenney JR, Jr., Glenney P (1985) Comparison of Ca++-regulated events in the intestinal brush border. *J Cell Biol* 100(3):754–763.
41. Schwartz N, et al. (1999) Ischemia activates actin depolymerizing factor: Role in proximal tubule microvillar actin alterations. *Am J Physiol* 276(4 Pt 2):F544–F551.
42. Ashworth SL, Sandoval RM, Hosford M, Bamburg JR, Molitoris BA (2001) Ischemic injury induces ADF relocalization to the apical domain of rat proximal tubule cells. *Am J Physiol Renal Physiol* 280(5):F886–F894.
43. Revenu C, et al. (2012) A new role for the architecture of microvillar actin bundles in apical retention of membrane proteins. *Mol Biol Cell* 23(2):324–336.
44. McConnell RE, Benesh AE, Mao S, Tabb DL, Tyska MJ (2011) Proteomic analysis of the enterocyte brush border. *Am J Physiol Gastrointest Liver Physiol* 300(5):G914–G926.
45. Haik BG, Zimny ML (1977) Scanning electron microscopy of corneal wound healing in the rabbit. *Invest Ophthalmol Vis Sci* 16(9):787–796.
46. Oganesian A, et al. (1997) Scanning and transmission electron microscopic findings during RPE wound healing in vivo. *Int Ophthalmol* 21(3):165–175.
47. Sacco O, et al. (2004) Epithelial cells and fibroblasts: Structural repair and remodelling in the airways. *Paediatr Respir Rev* 5(Suppl A):S35–40.
48. Revenu C, Gilmour D (2009) EMT 2.0: Shaping epithelia through collective migration. *Curr Opin Genet Dev* 19(4):338–342.
49. Raucher D, Sheetz MP (2000) Cell spreading and lamellipodial extension rate is regulated by membrane tension. *J Cell Biol* 148(1):127–136.
50. Dai J, Sheetz MP (1999) Membrane tether formation from blebbing cells. *Biophys J* 77(6):3363–3370.
51. Nambiar R, McConnell RE, Tyska MJ (2009) Control of cell membrane tension by myosin-I. *Proc Natl Acad Sci USA* 106(29):11972–11977.
52. Boulant S, Kural C, Zeeh J-C, Ubelmann F, Kirchhausen T (2011) Actin dynamics counteract membrane tension during clathrin-mediated endocytosis. *Nat Cell Biol* 13(9):1124–1131.
53. Morris CE, Homann U (2001) Cell surface area regulation and membrane tension. *J Membr Biol* 179(2):79–102.
54. Sinha B, et al. (2011) Cells respond to mechanical stress by rapid disassembly of caveolae. *Cell* 144(3):402–413.
55. Northrop J, et al. (1986) Different calcium dependence of the capping and cutting activities of villin. *J Biol Chem* 261(20):9274–9281.
56. Kiuchi T, Nagai T, Ohashi K, Mizuno K (2011) Measurements of spatiotemporal changes in G-actin concentration reveal its effect on stimulus-induced actin assembly and lamellipodium extension. *J Cell Biol* 193(2):365–380.
57. Kiuchi T, Ohashi K, Kurita S, Mizuno K (2007) Cofilin promotes stimulus-induced lamellipodium formation by generating an abundant supply of actin monomers. *J Cell Biol* 177(3):465–476.
58. Bronson SK, et al. (1996) Single-copy transgenic mice with chosen-site integration. *Proc Natl Acad Sci USA* 93(17):9067–9072.
59. Boulanger J, et al. (2010) Patch-based nonlocal functional for denoising fluorescence microscopy image sequences. *IEEE Trans Med Imaging* 29(2):442–454.